

Forbush decreases at a middle latitude neutron monitor: relations to geomagnetic activity and to interplanetary plasma structures

I. Parnahaj¹ · K. Kudela²

Received: 13 February 2015 / Accepted: 15 August 2015
© Springer Science+Business Media Dordrecht 2015

Abstract Results of statistical study on relations between Forbush decreases (FDs) as observed at a middle-latitude, high mountain cosmic ray (CR) neutron monitor (NM), and the geomagnetic storms (GS), as well as on connections of FDs to interplanetary plasma structures, are presented. Study confirms and extends (until 2014) earlier results based on NM data from different geomagnetic cut-off positions and covering earlier periods, namely that FDs associated with halo coronal mass ejections (CMEs) and those related with the shocks correspond to higher amplitudes of FDs than those without the mentioned features.

Keywords Forbush decrease · Geomagnetic storm · Coronal mass ejection · Interplanetary coronal mass ejection · Solar wind · Interplanetary magnetic field · Interplanetary shock · Magnetic cloud · Bidirectional suprathermal electron streaming

1 Introduction

For study of galactic cosmic ray (GCR) flux modulation (reviewed e.g. by Venkatesan and Badruddin 1990) NMs are frequently used. Rapid decreases followed by more gradual recovery in GCR flux named as FDs (Forbush 1937) are usually related to interplanetary (IP) coronal mass ejection (ICME) passing the Earth's orbit. Often, but not always, FDs are accompanied by GS. Rather complicated relationship

between FD and GS is reported e.g. by Kudela and Brenkus (2004), Kane (2010). GS can be classified using the Dst index (e.g. Sugiura 1964; Rockenbach et al. 2011).

CME is a giant eruption of plasma and magnetic field from the Sun with mass $> 10^{13}$ kg and speed of several thousand km/s (more e.g. in Howard 2014). Cane (2000) summarized the CME effects on particles and discussed the mechanisms behind. Study of CME evolution (observed by LASCO) during the cycle 23 and relation to GCR (observed by Climax NM until 2006) can be found e.g. in Lara et al. (2005). Arunbabu et al. (2013) report that primary contributors to FDs at high rigidities are the Earth-directed CMEs.

Halo CMEs are those completely encircling the Sun. Partial halo CMEs have width between 120° and 360° (Gopalswamy 2009). Halo CMEs play important role in producing large FDs. Verma et al. (2009) using Oulu NM data report that halo CMEs associated with X-ray solar flares and related to IP shocks are responsible for large FDs and GSs. ICMEs are IP counterparts of the CMEs. Their common signatures are described e.g. by Richardson et al. (2006). Connections between FD magnitude and CME, ICME, as well as with solar wind (SW) parameters are discussed for 1996–2011 by Belov et al. (2014). Mustajab and Badruddin (2013) and Kumar and Badruddin (2014) studied the relative geoeffectiveness of various IP structures and features associated with ICMEs and GCR modulation. Shrivastava et al. (2011) found that 63 % of solar flares associated with halo CMEs and FDs occur in the western hemisphere. Occurrence of FDs during the passage of > 300 ICMEs in the period 1995–2009 was found in 80 % cases (Richardson and Cane 2011).

When ICME has a speed overwhelming that of the sound of IP medium where ICME moves, a fast shock wave forms ahead of ICME. A turbulent sheath region created between shock and ICME can also cause intense GS. IP shocks arise

✉ K. Kudela
kkudela@kosice.upjs.sk

¹ Faculty of Science, Pavol Jozef Safarik University, Kosice, Slovakia

² Institute of Experimental Physics, Slovak Academy of Sciences, Kosice, Slovakia

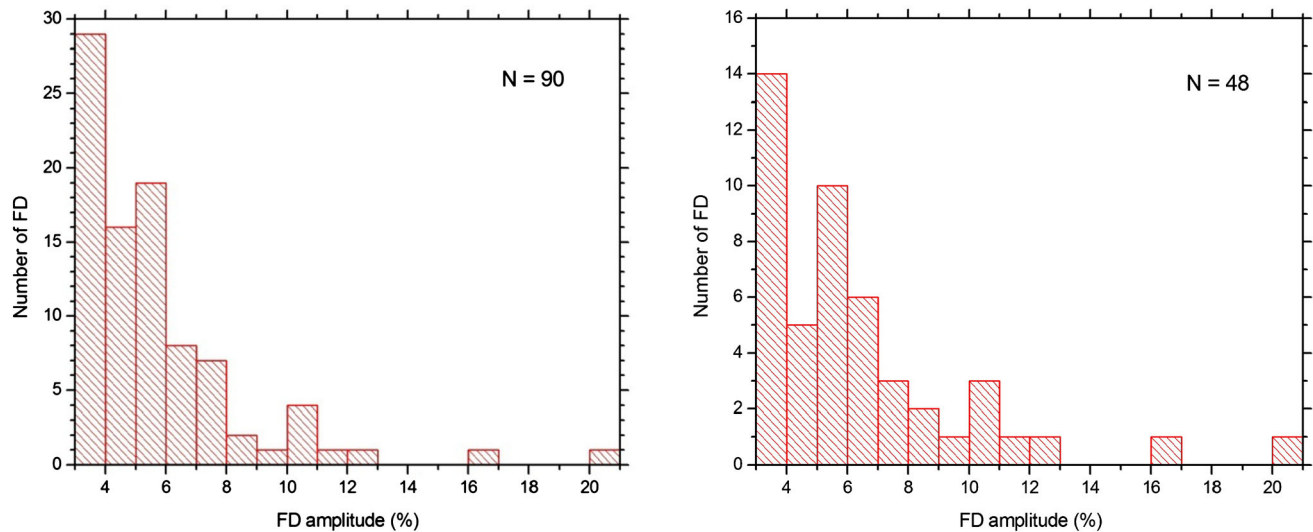


Fig. 1 Histograms of all FD amplitudes (*left panel*) and of FD amplitudes for events when information about associated IP structures (ICME, halo/non halo CME, shock, MC, BDE) are available

from a variety of sources (e.g. Borrini et al. 1982) and have a significant impact on geomagnetic activity (Mays et al. 2007). Characteristics of IP shocks have been studied e.g. in Gopalswamy et al. (2010), Howard and Tappin (2005). Numerical simulation shows that ICMEs and shocks follow different evolutions in IP medium (González-Esparza et al. 2003). The magnetic structure inside an ICME cloud is quite variable. Highly structured helical magnetic field observed within ICMEs, a magnetic cloud (MC) defined in Burlaga et al. (1981), is large configuration observed in IP space with signatures as enhanced interplanetary magnetic field (IMF) strength, smoothly rotating magnetic field vector and low plasma temperature (Osherovich and Burlaga 1997; Burlaga et al. 1990). The MCs—a special type of CME (Kilpua et al. 2013; Richardson and Cane 2004) play an important role in producing GS with impacts on the Earth (Wu et al. 2013; Farrugia et al. 2013). Cane et al. (1997) analyzing > 60 MeV particles on Helios 1, 2 reported no clear evidence that particle behavior depends on whether or not an ejecta is associated with MC. Recently Belov et al. (2015) indicated dependence of MC effect in CR density (FDs) on the size of MC.

Bidirectional electron streamings (BDE) are events with suprathermal electrons streaming parallel/anti-parallel to IMF. BDEs are interpreted as formation of closed loops of IMF within CME returning to the solar corona along both directions with origin in footpoints of ICME still anchored back to the Sun (Xie et al. 2000; Sergeev et al. 2001).

Here the results of statistical study on relationships between FDs amplitude, and interplanetary/geomagnetic characteristics using data from catalogue of CMEs, ICMEs, Dst list, OMNIWEB NASA site and ACE data, are presented. In several statistical studies of similar type there have been

used data covering intervals until 2006 (e.g. Blanco et al. 2013; Shrivastava et al. 2011) or until 2010 (Belov et al. 2015). FDs have different energy spectra and different amplitude of decreases are observed at different cut-off positions (e.g. Ahluwalia et al. 2014; Grigoryev et al. 2014). We use only large FDs observed at a high elevation middle cut-off rigidity NM, Lomnický stit (LS, $R_c = 3.84$ GV, $h = 2634$ masl) and cover the interval 1996–2014. After short checking the relations of FDs to GSs during 1982–2014, we present FDs amplitude in dependence on angular size of CMEs, on the occurrence of shocks, on acceleration/deceleration of CMEs and on velocity of motion of the structures in IP medium.

2 Data

Starting point was FD catalogue—a list of 90 FDs from NM at LS for period 1982–2014, added by information about associated GSs (from WDC for Geomagnetism in Kyoto (<http://wdc.kugi.kyoto-u.ac.jp/dstdir/>), solar wind speed (V_{SW}) and IMF. Out of 90 FDs with the amplitude $> 3\%$ we selected 48 events for the studied period when information about ICME is available. Distributions of FD amplitudes used in further study is in Fig. 1.

Along with IMF and SW data from (<http://omniweb.gsfc.nasa.gov>) we used: data of CME from LASCO CME list (http://cdaw.gsfc.nasa.gov/CME_list/); data of Near-Earth ICME from ACE list (Richardson and Cane 2007) (<http://www.srl.caltech.edu/ACE/ASC/DATA/level3/icmetable2.htm>). List contains information about time of disturbance typically related to the arrival of a shock or ICME leading edge at Earth, characteristics of ICME

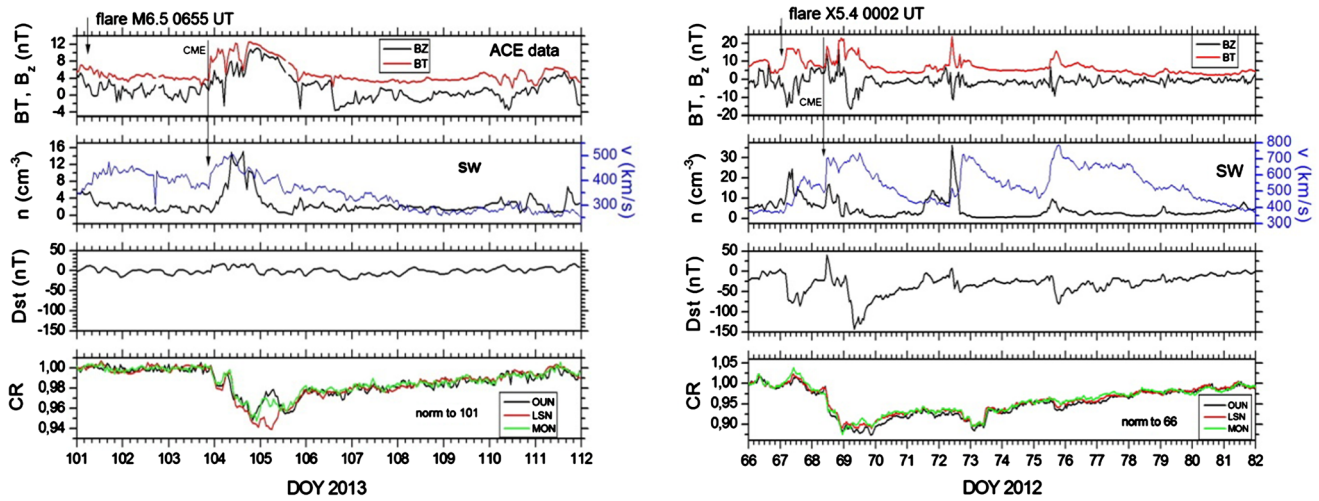


Fig. 2 Examples of different relations between CR decreases and geomagnetic activity: *left panel* for (11.4.-21.4.2013) and *right panel* for (6.3.-21.3.2012)

Table 1 Distribution of GSs for different FD amplitude threshold. Classification of storms is done according to Rockenbach et al. (2011)

	$3 \leq \text{FD} < 5$	$5 \leq \text{FD} < 7$	$7 \leq \text{FD} < 9$	$9 \leq \text{FD} < 11$	$11 \leq \text{FD}$
Events	45	27	9	5	4
Super storms	0.0 % (0)	3.7 % (1)	22.2 % (2)	40.0 % (2)	25.0 % (1)
Intense storms	13.3 % (6)	40.8 % (11)	55.6 % (5)	20.0 % (1)	50.0 % (2)
Moderate storms	40.0 % (18)	33.3 % (9)	11.1 % (1)	40.0 % (2)	25.0 % (1)
No storms	46.7 % (21)	22.2 % (6)	11.1 % (1)	0.0 % (0)	0.0 % (0)

cloud, and CME associated with ICME. Latter information helped us to assign the associated CME from LASCO CME list. ICME list was supplemented by information about interplanetary shocks from (www.ssg.sr.unh.edu/mag/ace/ACELists/obs_list.html) and (<http://umtof.umd.edu/pm/FIGS.HTML>). Thus the catalogues allowed us to split the events according to halo CMEs, shocks, MCs, BDEs and to provide statistical studies on various selections.

3 Forbush decreases and geomagnetic storms

Figure 2 illustrates the complexity of relations between FDs and GSs. Both events are related to the halo CMEs. Hourly averages from SWEPAM and the MAG on board ACE spacecraft (SW and IMF data), Kyoto Dst data, and CR intensity data from three European NMs with different geomagnetic cut-off rigidity (Oulu, Moscow and Lomnický štít), normalized for the first day, are used.

While CR decrease in left panel is not associated with clear Dst depression, in right panel it is. B_z of IMF is positive on the left panel, while on the right panel B_z is strongly negative. Halo CME on the left panel resulting from a M6.5 X-ray flare at 6:55 UT (DOY 101) located at N09E12 with

speed of 985.8 km/s, acceleration -27.13 m/s^2 and travel time 63.5 hours. Halo CME on the right panel resulted from X5.4 X-ray flare at 0:02 UT (DOY 67) located at N17E27, with speed of 2568.5 km/s, acceleration 47.43 m/s^2 and travel time 35 hours. The arrival time of CME is accompanied by a sharp increase in density and speed of SW (right event in long lasting recovery phase shows two more Dst depressions corresponding to SW speed and density increases and CR decreases).

We examined relations between FDs (as observed at NM LS), Dst depressions and interplanetary parameters for the period 1982–2014. Table 1 shows the distribution of GSs accompanying the FDs above a given threshold. Stronger FDs seem to be associated with stronger GSs. However the linear correlation coefficient between FD amplitude and Dst is only $r = -0.52$ (scatter plot is not shown here). Figure 3 presents comparison of relations between the FD amplitude as well as between the corresponding Dst min, and the values V_{sw} , IMF magnitude and its B_z component.

While the correlation coefficients of FD amplitude as well as of Dst min versus solar wind speed are comparable (upper panel), the binding of FD and of Dst min to the IMF as well as to its north-south component is different (middle and low panel): significantly higher is the correlation between Dst min and IMF magnitude and its B_z component,

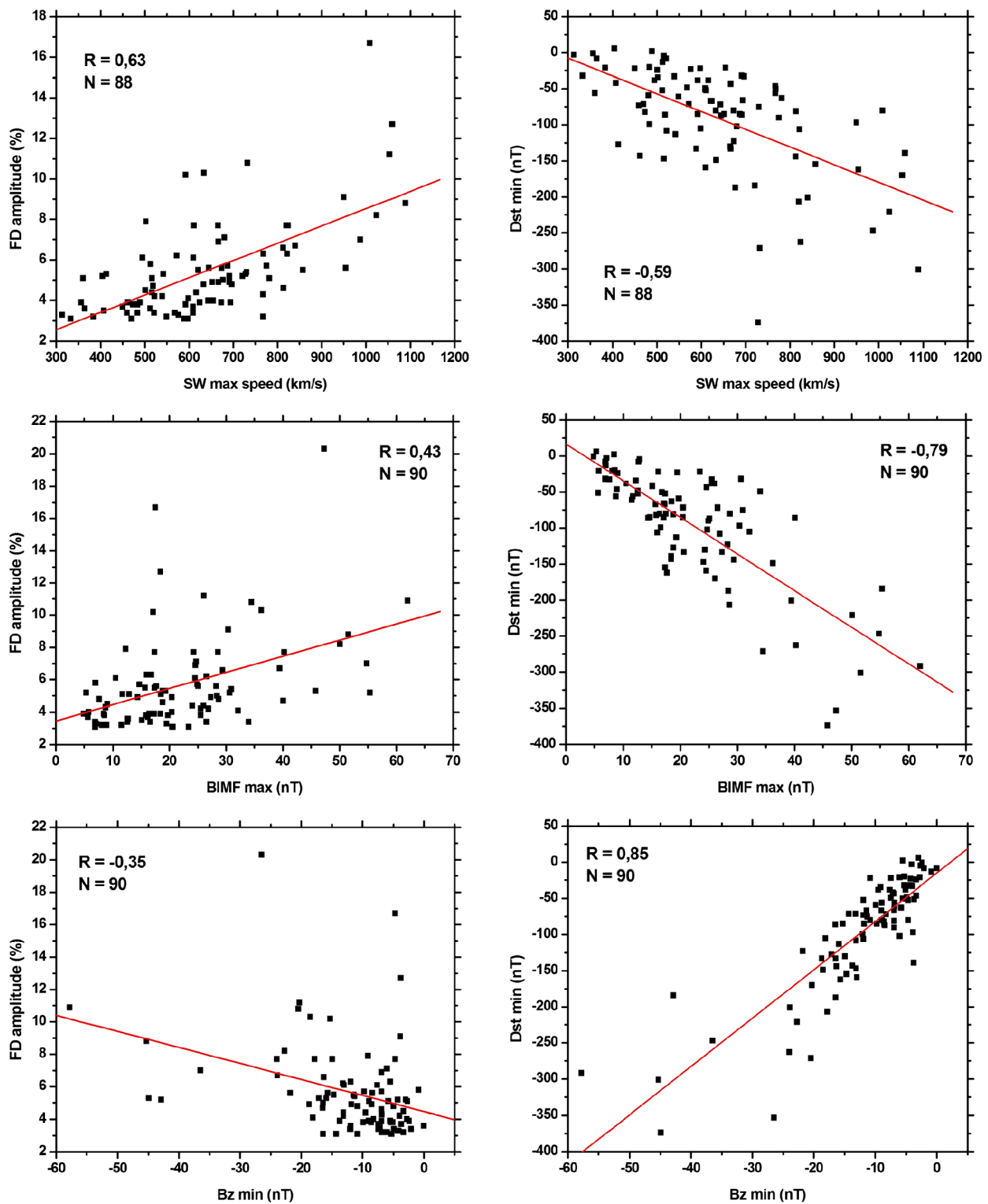


Fig. 3 Scatter plots of amplitude of FDs (*left panels*) and Dst min (*right panels*) vs. SW max speed, IMF and B_z min component of IMF

than the correlations between FD amplitude and these parameters. It confirms previous results about geoefficiency of CMEs (e.g. Badruddin and Kumar 2015) with the extension until year 2014.

One of possible physical quantities responsible for the production of stronger FDs is high speed of CME. Correlation coefficient between FD amplitude and CME speed is $r = 0.63$. CMEs with higher speeds can produce stronger

Table 2 Averaged amplitude of various parameters corresponding to different ranges of FD amplitude: V_{cme} —CME speed (km/s), a —acceleration of CME (m/s^2), V_{icme} —ICME speed (km/s), B_{icme} —

IMF strength in the ICME (nT), V_{trans} —mean transit speed of ICME at 1 AU (km/s), B_{imf} —IMF (nT), V_{sw} —SW speed (km/s)

FD (%)	Parameters							
	V_{cme}	a	V_{icme}	B_{icme}	V_{trans}	Dst	B_{imf}	V_{sw}
$3 \leq FD < 6$	912.07	-2.11	513.10	12.45	732.00	-88.90	23.45	599.41
$6 \leq FD < 9$	1268.36	-5.74	631.82	14.82	1016.90	-166.36	34.76	805.45
$9 \leq FD$	1795.50	-25.68	796.25	15.25	1321.25	-193.88	34.05	906.17

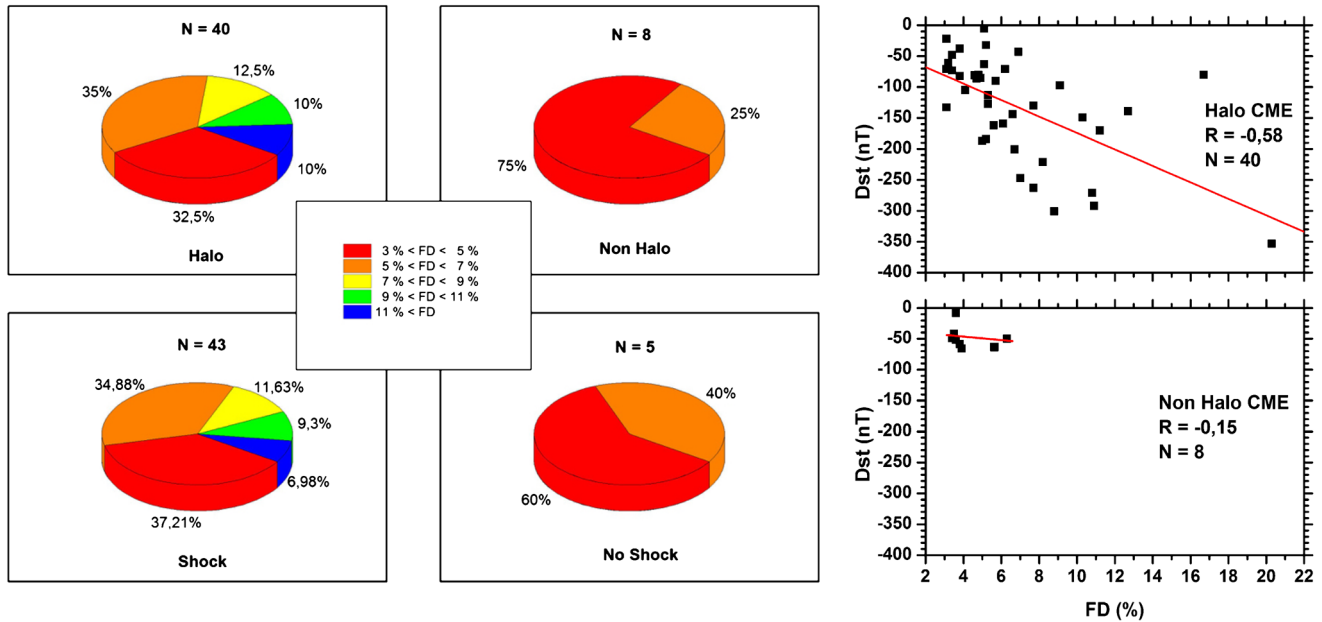


Fig. 4 Left: distribution of FD amplitude for ICMEs associated with halo CMEs and with shocks. Right: scatter plots of FD amplitude vs. Dst for Halo and Non Halo events

FDs, slower CMEs (speeds ~ 500 km/s) do not lead to a significant decrease in CR flux. ICME speed profile is highly dependent on the initial speed of the CME (Gopalswamy et al. 2000), but the changes of ICME speed during propagation in IP space are not under the control of initial speed of CME. The transition ICME speed (average speed of ICME when they arrive to the Earth) and the CME speed for the events selected here has correlation coefficient $r = 0.69$ —consistent with the result of Belov et al. (2014).

4 FDs and interplanetary plasma structures

For 48 FDs (distribution Fig. 1, right) when the parameters of IP structures (CME, shocks) are adjusted, Table 2 presents the average values for different FD amplitude ranges. For each event the extremal value of IP parameters is found and averaged in the corresponding FD bin.

Tendency of increase in velocities of plasma structures, namely V_{cme} , V_{trans} and V_{sw} with FDs amplitude is apparent.

Distribution of amplitudes of 48 FD events during 1996–2014 when accompanying CME and shock/no shock event was adjusted, is plotted in Fig. 4.

It is apparent that the width of CMEs and the occurrence of shock play the key role in producing stronger FDs. Stronger FDs are observed in association with halo CMEs. It is consistent with (Shrivastava et al. 2011—analysis of Oulu data for period 2001–2006). Figure 5 presents the relations of FD amplitude to selected parameters of the CME/ICME propagating from the solar surface.

Based on large amount of FDs for the period before 2011 Belov et al. (2014) found difference in the distribution of angular size of CMEs for events with FD and without FD by analyzing the non-recurrent FDs. Here the selection of events is coming out from FDs $> 3\%$. Left upper panel of Fig. 5 is consistent with that result, although statistics is lower.

The amplitude of FD as observed at Oulu NM for the events before 2006 was found to be organized according to

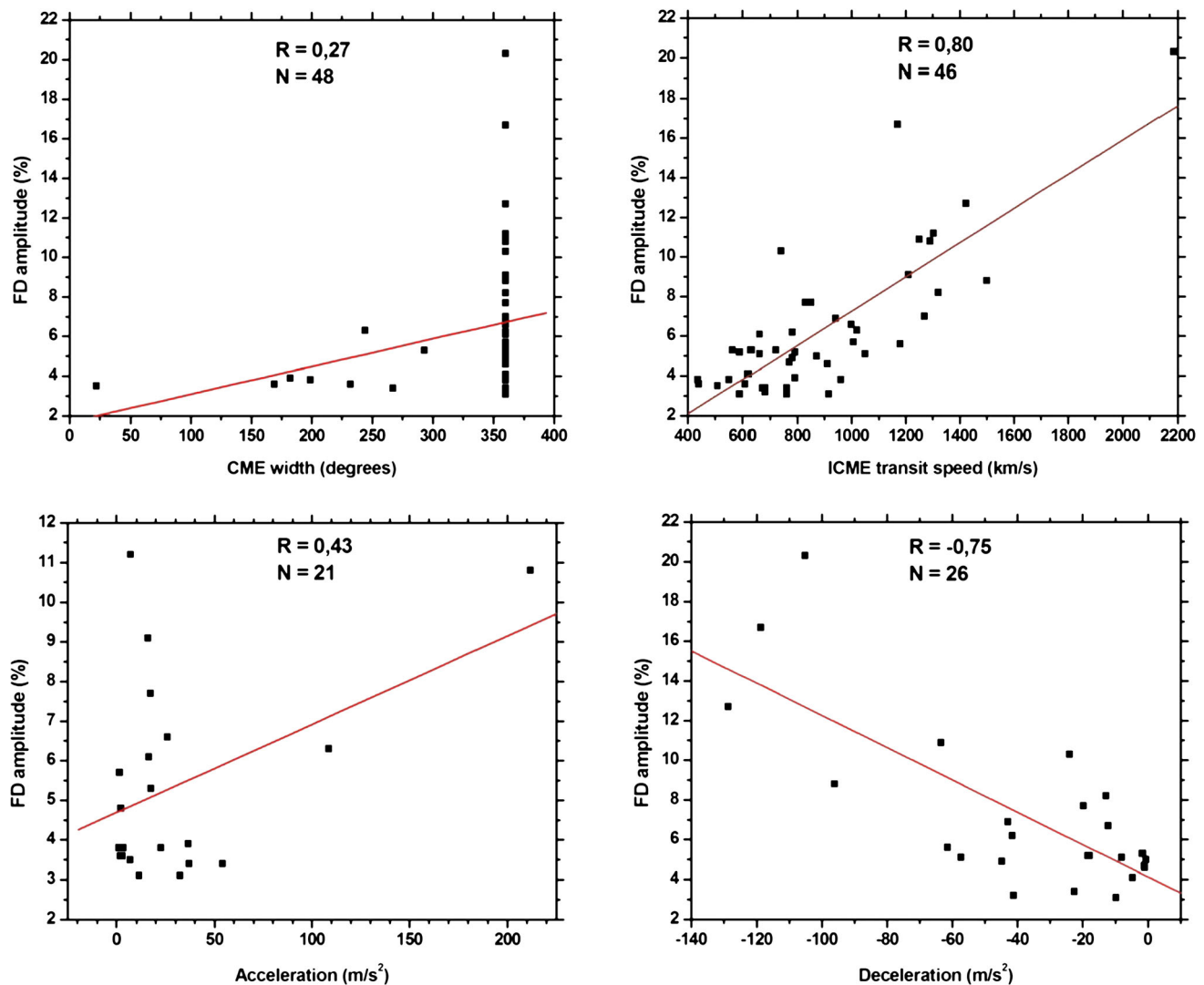


Fig. 5 Scatter plots of FD amplitudes vs. CME width, ICME transit speed and acceleration/deceleration of CMEs

ICME speed (Blanco et al. 2013). Such tendency is here confirmed for longer time period and at higher geomagnetic cut-off position of NM (Fig. 5, upper right).

Fast ICMEs are decelerated and slow ICMEs are accelerated due to their interaction with the SW (Jones et al. 2007). Higher correlation coefficient (negative) is seen between FD amplitudes and deceleration of CMEs than between FD amplitudes and CME acceleration (Fig. 5, lower panels). It confirms the results by Blanco et al. (2013) at lower geomagnetic cut-off rigidity NM. Deceleration of CME can play more important role in producing higher FD amplitudes than acceleration of CMEs. This can be explained by interaction between the ICME and SW, where the effective energy between ICME and SW is exchanged. It was shown that the significant momentum changes between these interacting structures can cause the deceleration of ICME and the forces responsible for the deceleration are aerodynamic

drag, gravitation of the Sun and the tension of magnetic field (Shen et al. 2012).

To understand the influence of structures as BDEs and MCs are, in producing the FDs, the events were splitted into various combinations with shocks and with the angular width of ICMEs. Table 3 presents averaged values of FD amplitude as well as of corresponding values of Dst min, IMF magnitude and solar wind speed for various combinations of IP structures.

Although the statistics is not high, the tendencies in FD magn as well as in Dst min, V_{sw} max and B_{imf} max is seen from that table: (i) occurrence of shock and wide ICME (halo) in combination with MC provides the highest averaged FD amplitude; the same is valid for |Dst min|, V_{sw} and B_{imf} ; (ii) narrow ICMEs or absence of the shock is accompanied by smaller FD and |Dst min| than the events with the halo ICME accompanied by the shock; (iii) the smallest

Table 3 Averaged values of maxima (for Dst minima) in various parameters associated with different IP structures. Numbers of events are in the brackets

ICME	FD magn	Dst min	V_{sw} max	B_{imf} max
Halo (40/48)	6.79	-131.48	713.58	29.03
Non Halo (8/48)	4.18	-87.50	570.50	21.74
Shock (43/48)	6.32	-132.35	702.29	29.16
No Shock (5/48)	4.58	-53.60	577.20	16.20
BDE (45/48)	6.50	-128.58	703.74	28.67
BDE and Shock (40/45)	6.48	-137.95	720.39	30.23
BDE and Halo (39/45)	6.82	-131.95	718.22	29.27
BDE and Shock and Halo (36/45)	6.68	-138.31	722.82	30.43
MC (25/48)	6.40	-147.08	689.17	28.52
MC and Shock (22/25)	6.69	-160.50	717.62	30.21
MC and Halo (20/25)	6.87	-156.70	720.32	30.27
MC and Shock and Halo (18/25)	7.13	-169.28	746.88	32.04
Halo or Shock (46/48)	6.47	-127.35	699.82	28.26
Halo and Shock (37/48)	6.64	-137.62	717.66	30.13
Non Halo and No Shock (2/48)	3.65	-50.50	444.00	17.40
Non Halo or No Shock (11/48)	5.36	-78.82	596.55	20.01
BDE and Non Halo and No Shock (2/45)	3.65	-50.50	444.00	17.40
MC and Non Halo and No Shock (1/25)	3.80	-59.00	481.00	19.70

FDs occur for the events with narrow ICME unaccompanied by the shock (2 events, also the smallest $|Dst\ min|$, V_{sw} and B_{imf}); (iv) BDE events as well as MC events themselves either without halo ICME or without shock correspond to small FD amplitude (low statistics). However, it has to be mentioned here, that the table provides just rough characteristics, since we do not distinguish the two-step FDs (associated with ejecta and with the shock, respectively) and we take such events as a single one.

5 Summary

Results of statistical study of FDs ($> 3\%$) observed at a middle-latitude neutron monitor during 1982–2014, confirm those reported in earlier studies based on different geomagnetic positions of NMs and extend them for part of the solar cycle 24. They indicate that:

- FDs, although not always accompanied by GSs, tend to correlate its amplitude with the Dst min value (e.g. no $FD < 5\%$ is accompanied by geomagnetic super storm; each $FD > 9\%$ is accompanied by at least moderate GS). Contrary to FD, the strength of GS is controlled by B_z and by IMF magnitude.
- The amplitude of FD events associated by CMEs is increasing with the speed of motion of IP structures and with the magnitude of magnetic field inside the CME.
- Most important parameters of CMEs/ICMEs controlling the depth of FDs are (i) the angular size of CME and (ii) presence of the shock. Narrow ICMEs and absence of the shocks significantly decrease FD amplitude. Although

MC in coincidence with halo CME and with the shock indicate high value of FD amplitude, MC themselves probably do not produce strong FD (low statistics). The same is valid for BDE events.

- Deceleration of CME seems to be a better producer of stronger FDs than the acceleration of CMEs.

Further progress in understanding the efficiency of IP irregular plasma structures emitted from the Sun on the decreases of CR as measured on Earth's surface, requires more extensive study using data from *all CMEs* and data from various NMs and muon telescopes. One such work in that direction is under preparation.

Acknowledgements VEGA 2/0040/13 and VVGS-PF-2014-445 are acknowledged for support. The CME catalog used is generated and maintained at the CDAW Data Center by NASA and The Catholic University of America in cooperation with the Naval Research Laboratory. SOHO is a project of international cooperation between ESA and NASA.

References

- Ahluwalia, H.S., Alania, M.V., Wawrzynczak, A., Ygbuhay, R.C., Fikani, M.M.: May 2005 halo CMEs and galactic cosmic ray flux changes at Earth's orbit. *Sol. Phys.* **289**, 1763–1782 (2014)
- Arunbabu, K.P., Antia, H.M., Dugad, S.R., Gupta, S.K., Hayashi, Y., Kawakami, S., Mohanty, P.K., Nonaka, T., Oshima, A., Subramanian, P.: High-rigidity Forbush decreases: due to CMEs or shocks? *Astron. Astrophys.* **555**, A139 (2013)
- Badruddin, Kumar, A.: Study of the Forbush decreases, geomagnetic storms, and ground-level enhancements in selected intervals and their space weather implications. *Sol. Phys.* **290**, 1271–1283 (2015). doi:[10.1007/s11207-015-0665-4](https://doi.org/10.1007/s11207-015-0665-4)

- Belov, A., Abunin, A., Abunina, M., Eroshenko, E., Oleneva, V., Yanke, V., Papaioannou, A., Mavromichalaki, H., Gopalswamy, N., Yashiro, S.: Coronal mass ejections and non-recurrent Forbush decreases. *Sol. Phys.* (2014). doi:[10.1007/s11207-014-0534-6](https://doi.org/10.1007/s11207-014-0534-6)
- Belov, A., Abunin, A., Abunina, A., Eroshenko, E., Oleneva, V., Yanke, V., Papaioannou, A., Mavromichalaki, H.: Galactic cosmic ray density variations in magnetic clouds. *Sol. Phys.* **290**, 1429–1444 (2015)
- Blanco, J.J., Catalán, E., Hidalgo, M.A., Medina, J., García, O., Rodríguez-Pacheco, J.: Observable effects of interplanetary coronal mass ejections on ground level neutron monitor count rates. *Sol. Phys.* **284**(1), 167–178 (2013). doi:[10.1007/s11207-013-0256-1](https://doi.org/10.1007/s11207-013-0256-1)
- Borini, G., Gosling, J.T., Bame, S.J.: An analysis of shock wave disturbances observed at 1 AU from 1971 through 1978. *J. Geophys. Res.* **87**, 4365 (1982)
- Burlaga, L.F., Sittler, E., Mariani, F., Schwenn, R.: *J. Geophys. Res.* **86**(A8), 6673 (1981)
- Burlaga, L.F., Lepping, R., Jones, J.: Global configuration of a magnetic cloud. In: Russell, C.T., Priest, E.R., Lee, L.C. (eds.) *Physics of Flux Ropes*. *Geophys. Monogr. Ser.*, vol. 58, pp. 373–377. Am. Geophys. Union, Washington (1990)
- Cane, H.V.: Coronal mass ejections and Forbush decreases. *Space Sci. Rev.* **93**, 55–77 (2000)
- Cane, H.V., Richardson, I.G., Wibberenz, G.: Helios I and 2 observations of particle decreases, ejecta, and magnetic clouds. *J. Geophys. Res.* **102**(A4), 7075–7086 (1997)
- Farrugia, C.J., Erkaev, N.V., Jordanova, V.K., Lugaz, N., Sandholt, P.E., Mühlbacher, S., Torbert, R.B.: Features of the interaction of interplanetary coronal mass ejections/magnetic clouds with the Earth's magnetosphere. *J. Atmos. Sol.-Terr. Phys.* **99**, 14–26 (2013). doi:[10.1016/j.jastp.2012.11.014](https://doi.org/10.1016/j.jastp.2012.11.014)
- Forbush, S.E.: On the effects in the cosmic ray intensity observed during magnetic storms. *Phys. Rev.* **51**, 1108–1109 (1937)
- González-Esparza, J.A., Lara, A., Santillán, A., Gopalswamy, N.: A numerical study on the evolution of CMEs and shocks in the interplanetary medium. In: *Solar Wind Ten: Proceedings of the Tenth International Solar Wind Conference*. AIP Conference Proceedings, vol. 679, pp. 206–209 (2003). doi:[10.1063/1.1618578](https://doi.org/10.1063/1.1618578)
- Gopalswamy, N.: Halo coronal mass ejections and geomagnetic storms. *Earth Planets Space* **61**, 1–3 (2009)
- Gopalswamy, N., Lara, A., Lepping, R.P., Kaiser, M.L., Berdichevsky, D., St. Cyr, O.C.: *Geophys. Res. Lett.* **27**, 145 (2000)
- Gopalswamy, N., Xie, H., Mäkelä, P., Akiyama, S., Yashiro, S., Kaiser, M.L., Howard, R.A., Bougeret, J.-L.: Interplanetary shocks lacking type II radio bursts. *Astrophys. J.* **710**(2), 1111 (2010). doi:[10.1088/0004-637X/710/2/1111](https://doi.org/10.1088/0004-637X/710/2/1111)
- Grigoryev, V.G., Starodubtsev, S.A., Isakov, D.D.: The energy spectrum of Forbush decreases during the growth phase of solar cycle 24. *Geomagn. Aeron.* **54**(3), 304–309 (2014)
- Howard, T.: *Space Weather and Coronal Mass Ejections*. Springer, Berlin (2014)
- Howard, T.A., Tappin, S.J.: Statistical survey of earthbound interplanetary shocks, associated coronal mass ejections and their space weather consequences. *Astron. Astrophys.* **440**, 373–383 (2005). doi:[10.1051/0004-6361:20053109](https://doi.org/10.1051/0004-6361:20053109)
- Jones, R.A., Breen, A.R., Fallows, R.A., Canals, A., Bisi, M.M., Lawrence, G.: Interaction between coronal mass ejections and the solar wind. *J. Geophys. Res.* **112**, A08107 (2007). doi:[10.1029/2006JA011875](https://doi.org/10.1029/2006JA011875)
- Kane, R.P.: Severe geomagnetic storms and Forbush decreases: interplanetary relationships reexamined. *Ann. Geophys.* **28**, 479–489 (2010)
- Kilpua, E.K.J., Isavnin, A., Vourlidas, A., Koskinen, H.E.J., Rodriguez, L.: On the relationship between interplanetary coronal mass ejections and magnetic clouds. *Ann. Geophys.* **31**, 1251–1265 (2013). doi:[10.5194/angeo-31-1251-2013](https://doi.org/10.5194/angeo-31-1251-2013)
- Kudela, K., Brenkus, R.: Cosmic ray decreases and geomagnetic activity: list of events 1982–2002. *J. Atmos. Sol.-Terr. Phys.* **66**(13–14), 1121–1126 (2004)
- Kumar, A., Badruddin: Interplanetary coronal mass ejections, associated features, and transient modulation of galactic cosmic rays. *Sol. Phys.* **289**(6), 2177–2205 (2014). doi:[10.1007/s11207-013-0465-7](https://doi.org/10.1007/s11207-013-0465-7)
- Lara, A., Gopalswamy, N., Caballero-López, R.A., Yashiro, S., Xie, H., Valdés-Galicia, J.F.: Coronal mass ejections and galactic cosmic-ray modulation. *Astrophys. J.* **625**, 441–450 (2005)
- Mays, M.L., Horton, W., Kozyra, J., Zurbuchen, T.H., Huang, C., Spencer, E.: Effect of interplanetary shocks on the AL and Dst indices. *Geophys. Res. Lett.* **34**, L11104 (2007). doi:[10.1029/2007GL029844](https://doi.org/10.1029/2007GL029844)
- Mustajab, F., Badruddin: Relative geo-effectiveness of coronal mass ejections with distinct features in interplanetary space. *Planet. Space Sci.* **82–83**, 43–61 (2013). doi:[10.1016/j.pss.2013.03.011](https://doi.org/10.1016/j.pss.2013.03.011)
- Osherovich, V.A., Burlaga, L.F.: In: Crooker, N.U., Joselyn, J.A., Feynman, J. (eds.) *Magnetic Clouds*. *Geophysical Monogr. Ser.*, vol. 99, p. 157. Am. Geophys. Union, Washington (1997)
- Richardson, I.G., Cane, H.V.: The fraction of interplanetary coronal mass ejections that are magnetic clouds: evidence for a solar cycle variation. *Geophys. Res. Lett.* **31**(18) (2004). doi:[10.1029/2004GL020958](https://doi.org/10.1029/2004GL020958)
- Richardson, I.G., Cane, H.V.: Interplanetary coronal mass ejections during 1996–2007. In: *Proc. 30th Int., Cosmic Ray Conf., Merida, Mexico* (2007)
- Richardson, I.G., Cane, H.V.: Galactic cosmic ray intensity response to interplanetary coronal mass ejections/magnetic clouds in 1995–2009. *Sol. Phys.* **270**, 609–627 (2011). doi:[10.1007/s11207-011-9774-x](https://doi.org/10.1007/s11207-011-9774-x)
- Richardson, J.D., Liu, Y., Wang, C., Burlaga, L.: ICMs at very large distances. *Adv. Space Res.* **38**, 528 (2006). doi:[10.1016/j.asr.2005.06.049](https://doi.org/10.1016/j.asr.2005.06.049)
- Rockenbach, M., et al.: Geomagnetic storm's precursors observed from 2001 to 2007 with the global muon detector network (GMDN). *Geophys. Res. Lett.* **38**, L16108 (2011). doi:[10.1029/2011GL048556](https://doi.org/10.1029/2011GL048556)
- Sergeev, V.A., Baumjohann, W., Shiokawa, K.: Bi-directional electron distributions associated with near-tail flux transport. *Geophys. Res. Lett.* **28**(19), 3813–3816 (2001). doi:[10.1029/2001GL013334](https://doi.org/10.1029/2001GL013334)
- Shen, F., Wu, S.T., Feng, X., Wu, C.C.: Acceleration and deceleration of coronal mass ejections during propagation and interaction. *J. Geophys. Res.* **117**, A11101 (2012)
- Shrivastava, P.K., Jothe, M.K., Singh, M.: Longitudinal distribution of solar flares and their association with coronal mass ejections and Forbush decreases. *Sol. Phys.* **269**, 401–410 (2011)
- Sugiura, M.: Hourly Values of Equatorial Dst for the IGY. *Ann. Int. Geophys. Year*, vol. 35, p. 9. Pergamon Press, Oxford (1964)
- Venkatesan, D., Badruddin: Cosmic-ray intensity variations in the 3-dimensional heliosphere. *Space Sci. Rev.* **52**, 121–194 (1990)
- Verma, P.L., Tiwari, R.K., Kumar, Y., Nigam, S.K., Sharma, A.B., Khare, N.: Halo coronal mass ejections: the cause of large Forbush decreases and geomagnetic storms. In: *Proceedings of the 31st ICRC, Lodz, paper icrc0198* (2009)
- Wu, C.C., Gopalswamy, N., Lepping, R.P., Yashiro, S.: Characteristics of magnetic clouds and interplanetary coronal mass ejections which cause intense geomagnetic storms. *Terr. Atmos. Ocean. Sci.* **24**(2), 233–241 (2013). doi:[10.3319/TAO.2012.09.26.03\(SEC\)](https://doi.org/10.3319/TAO.2012.09.26.03(SEC))
- Xie, R.X., Fu, Q.J., Wang, M., Liu, Y.Y.: The generating region of bidirectional electron beams in the corona. *Sol. Phys.* **197**(2), 375–385 (2000). doi:[10.1023/A:1026541718129](https://doi.org/10.1023/A:1026541718129)